Sanchez-Paulete AR, Teijeira A, Quetglas JI, Rodriguez-Ruiz ME, Sanchez-Arraez A, Labiano S, Etxeberria I, Azpilikueta A, Bolanos E, Ballesteros-Briones MC, Casares N, Quezada SA, Berraondo P, Sancho D, Smerdou C, Melero I. Intratumoral immunotherapy with XCL1 and sFlt3L encoded in recombinant Semliki Forest Virus-derived vectors fosters dendritic cell-mediated T cell cross-priming. *Cancer Res*, 2018. 78(23): p. 6643-54.

Intratumoral immunotherapy with XCL1 and sFlt3L encoded in recombinant Semliki Forest Virus-derived vectors fosters dendritic cell-mediated T cell cross-priming

Alfonso R. Sánchez-Paulete[1], Álvaro Teijeira[1], José I. Quetglas[1], María E. Rodríguez-Ruiz[2], Álvaro Sánchez-Arráez[1], Sara Labiano[1], Iñaki Etxeberria[1], Arantza Azpilikueta[1], Elixabet Bolaños[1,3], María Cristina Ballesteros-Briones[4], Noelia Casares[1], Sergio A. Quezada[5], Pedro Berraondo[1,3], David Sancho[6], Cristian Smerdou[4]*, Ignacio Melero[1,2,3]*,+

1. Division of Immunology and Immunotherapy, Center for Applied Medical Research (CIMA), University of Navarra, and Instituto de Investigación Sanitaria de Navarra (IdISNA), Pamplona, Spain

2. University Clinic, University of Navarra and Instituto de Investigación Sanitaria de Navarra (IdISNA), Pamplona, Spain

3. CIBERONC, Instituto de Investigación Carlos III, Madrid, Spain

4. Division of Gene Therapy and regulation of gene expression, Center for Applied Medical Research (CIMA), University of Navarra, and Instituto de Investigación Sanitaria de Navarra (IdISNA), Pamplona, Spain

5. Cancer Immunology Unit, University College **London** Cancer Institute, University College **London**. London, UK.

6. Fundación Centro Nacional de Investigaciones Cardiovasculares Carlos III (CNIC), Madrid, Spain

*These authors share senior authorship

+Correspondence:

Ignacio Melero Bermejo, MD, PhD

Center for Applied Medical Research, Avenida Pío XII 55, Pamplona 31008, Spain

Telephone: +34 948 194 700 ext. 3031

Email address: imelero@unav.es

Running title (60 characters): Virally encoded XCL1 and sFlt3L for local immunotherapy

Keywords (5): Semliki Forest Virus, Cross-priming, Dendritic cell, Intratumoral Immunotherapy, Cancer Virotherapy

Word count:

Intro + Mat/Met + Results + Discussion = 4,049

Intro + Mat/Met + Results + Discussion + Figure Legends = 5,144

Figure count: 7 main figures, 7 supplementary figures and 1 supplementary material and methods

Conflicts of Interest disclosure: IM has served as a consultant for Bristol-Myers Squib, Roche-Genentech, Bayer, Alligator, Tusk, Bioncotech, Medimmune, Genmab, F-Star. IM receives commercial grants from Bristol Myers Squibb, Roche-Genentech and Alligator. SQ is a consultant for Tusk.

ABSTRACT

Multiple lines of evidence indicate a critical role for antigen cross-presentation by conventional BATF3-dependent type 1 classical dendritic cells (cDC1) in CD8-mediated antitumor immunity. Flt3L and XCL1 respectively constitute a key growth/differentiation factor and a potent and specific chemoattractant for cDC1. To exploit their antitumor functions in local immunotherapy, we prepared Semliki Forest Virus (SFV)-based vectors encoding XCL1 and soluble Flt3L (sFlt3L). These vectors readily conferred transgene expression to tumor cells in culture and when engrafted as subcutaneous mouse tumor models. In syngeneic mice, intratumoral injection of SFV-XCL1-sFlt3L (SFV-XF) delayed progression of MC38- and B16-derived tumors. Therapeutic activity was observed and exerted additive effects in combination with anti-PD-1, anti-CD137, or CTLA-4 immunostimulatory monoclonal antibodies. Therapeutic effects were abolished by CD8β T cell depletion and were enhanced by CD4 T cell depletion, but not by Treg pre-depletion with anti-CD25 mAb. Antitumor effects were also abolished in BATF3- and IFNAR-deficient mice. In B16-OVA tumors, SFV-XF increased the number of infiltrating CD8 T cells, including those recognizing OVA. Consistently, following intratumoral SFV-XF treatment courses, we observed increased BATF3-dependent cDC1 among B16-OVA tumor-infiltrating leukocytes. Such an intratumoral increase was not seen in MC38-derived tumors, but both resident and migratory cDC1 were boosted in SFV-XF-treated MC38 tumor-draining lymph nodes. In conclusion, viral gene transfer of sFlt3L and XCL1 is feasible, safe, and biologically active in mice, exerting antitumor effects that can be potentiated by CD4 T cell depletion.

Significance: Findings demonstrate that transgenic expression of sFLT3L and XCL1 in tumor cells mediates cross-priming of, and elicits potent antitumor activity from, CD8 T lymphocytes, particularly in combination with CD4 T cell depletion.

INTRODUCTION

Cancer immunotherapy is in the limelight of oncology therapeutics due to the efficacy of systemic administration of checkpoint inhibitors and chimeric antigen receptor-transduced T cells (1). Intratumoral approaches with immunotherapy agents are feasible (2), and include local administration of Toll-like receptor or STING agonists (3,4) and recombinant oncolytic viruses (5) or viral vectors (6). Most immunotherapy approaches necessarily rely on the activation of CD8 T lymphocytes by mature dendritic cells (DCs) presenting cognate tumor antigens (7). A subset of DCs dependent on the transcription factors BATF3 and IRF8 for their ontogeny is critical for the activation of CD8 T lymphocytes (8,9) and crucial for the antitumor efficacy of treatment with anti-PD1 and anti-CD137 mAbs in mouse models (10). BATF3-dependent DCs are also termed type 1 conventional DCs (cDC1s) and excel in uptaking antigens from dead cells and presenting their peptides on MHC-I molecules (cross-presentation), leading to the activation/expansion of specific cytotoxic T lymphocytes (cross-priming). Two subsets of mouse cDC1 have been identified. One of these resides in T-cell zones of lymphoid organs (CD11c$^+$CD8α$^+$CD103$^-$Clec9a$^+$) (11) and the other (CD11c$^+$CD8α$^-$CD103$^+$Clec9a$^+$) is deployed in peripheral tissues and migrates towards lymphoid tissue once activated (7,12). Migratory CD103$^+$ cDC1s have been observed to carry tumor antigen to tumor-draining lymph nodes for cross-presentation (10,13,14). Flt3L is a critical growth/differentiation factor for this DC subpopulation (15) and XCL1 a chemokine that chemoattracts cDC1s, which exclusively express the XCL1 receptor (XCR1) (16) to allow for cDC1 *rendezvous* with NK and CD8 T cells (17,18). cDC1s are endowed with abundant TLR3 expression that drives their activation/maturation once challenged with dsRNA denoting viral infection (19).

Local gene transfer into experimental tumors with Semliki Forest Virus (SFV)-derived vectors is feasible and has an attractive immunotherapeutic potential. Although SFV vectors are not replication-competent viruses, they induce catastrophic death of infected cells (20), release abundant viral dsRNA (21), induce local IFNα/β production (21), and are safe. Indeed, a vector

4

encoding IL-12 (SFV-IL12) is highly efficacious in murine (22) and woodchuck (23) models of cancer and synergizes with other immunotherapies such as treatment with anti-PD-1 (24) and anti-CD137 (25) immunomodulatory mAbs.

Transfection of sFlt3L (26) or XCL1 (27) into tumor cells has been previously tested in culture and *in vivo* with immunotherapy purposes, achieving excellent vaccination effects in the case of sFlt3L (26).

In this study, repeated injections of an SFV vector simultaneously expressing sFlt3L and XCL1 were tested in an attempt to attract and expand cDC1 cells, while killing a fraction of tumor cells and providing viral RNA-mediated activation of innate immunity (28). Partial antitumor activity was substantiated against transplantable established tumors. This antitumor effect was dependent on CD8 T cells and on the integrity of the BATF3 and IFNAR genes in tumor-bearing mice.

MATERIALS AND METHODS

Cell Lines and Culture Conditions

MC38 cells were a kind gift from Dr. Karl E. Hellström (University of Washington, Seattle, WA) in September 1998. B16-OVA cells were provided by Dr. Lieping Chen (Yale University, New Haven, CT) in November 2001. B16F10 cells were purchased from the ATCC in June 2006. CT26 cells were purchased from ATCC in 2011. These cell lines were authenticated by Idexx Radil (Case 6592-2012) in February 2012. Panc02 tumor tissue was obtained from the National Cancer Institute, DCTDC Tumor Repository (Frederick, MD, USA). A cell line was isolated from trypsinization of Panc02 grafted tumor tissue (29). MC38, PANC02, CT26, B16F10 and B16-OVA cells were cultured in RPMI medium (Gibco) supplemented with 10% decomplemented and filtered FBS (Sigma Aldrich), containing 50 μmol/L β-mercaptoethanol, 100 U/mL penicillin, and 100 μg/mL streptomycin (all from Gibco). Baby Hamster Kidney (BHK) cells were cultured in GMEM-BHK21 medium (Gibco) supplemented with 5% decomplemented and filtered FBS (Sigma Aldrich), containing 20 mM Hepes (Invitrogen), 10% Tryptose Phosphate Broth, 2 mM glutamine, 100 U/mL penicillin and 100 μg/mL streptomycin (all from Gibco). When indicated, BHK cells were cultured in CHO medium (Sigma) supplemented with the same components as indicated for BHK, save for the FBS. For infection, cells were incubated in MEM medium (Gibco) containing 0.2% bovine serum albumin (Sigma).

Functional assays for transgene products

BHK cells were infected with SFV vectors at an MOI of 10 as described above and incubated overnight in serum-free CHO medium (Sigma) for XCL1 bioactivity testing or GMEM BHK-21 (Gibco)

for Flt3L bioactivity testing. Supernatants were collected and kept frozen until use. For Flt3L testing, bone marrow cell suspensions were flushed out of hind limb bones and cultured in RPMI medium conditioned with 20% infected BHK-derived supernatants. After 9 days, classical BM-DC (CD11c$^+$CD11b$^+$) and plasmacytoid BM-DC (CD11c$^+$CD11b$^-$B220$^+$) cells were assessed by flow cytometry to demonstrate sFlt3L-dependent differentiation. For XCL1 testing, standard transwell chemotaxis assays were performed on iCD103 BM-DCs (30). 10^5 iCD103 cells were suspended in serum-free CHO medium and plated onto 5 μm transwell inserts (Costar). Cells were allowed to migrate for four hours toward infected BHK-derived supernatants and the total number of cells in the lower well was quantitated by flow cytometry.

Mice and *in vivo* tumor experiments

Experiments involving mice were carried out in the animal facility of the Center for Applied Medical Research (CIMA, Pamplona, Spain) under study approvals 150/12 and 082/16 from the University of Navarra Ethics Committee. C57Bl/6 *Batf3$^{tm1Kmm/J}$* (Batf3 KO)_(8), *Tmem173$^{gt/J}$* (STING KO) (31) and *IFN-α/bR$^{o/o}$* (IFNAR KO) (32) mice were bred at CIMA in specific pathogen-free conditions. C57Bl/6 mice were obtained from Envigo (Barcelona, Spain). Batf3 KO, STING KO and IFNAR KO mice were kindly provided, respectively, by Dr. Kenneth M. Murphy, Washington University, St. Louis, MO, by Dr. Gloria González Aseguinolaza (CIMA, Pamplona) and by Dr. Matthew Albert (Institut Pasteur, Paris). Cultured tumor cells were cultured and trypsinized for injection before reaching confluence. 5 x 10^5 MC38 or B16-OVA cells were injected subcutaneously in 50 μl PBS into the right flank of 6- to 12-week old mice. SFV viral particles (VPs) were diluted in PBS and kept ice-cold until administration. Intratumoral injection of 50 μl suspension containing 10^8 VPs or vehicle control was performed using 29G syringes and under inhalatory anesthesia. When indicated, 100 μg anti-CD137 (1D8) or anti-PD-1 (RMP1-14) were administered intraperitoneally (i.p.) in PBS. Depletion of lymphocyte subsets was performed by i.p. injection of anti-CD4 (GK1.5, Bioxcell, West Lebanon, NH), anti-CD8 (H35-17.2, in-

house) or anti-NK1.1 (PK136, in-house) mAbs. 200 µg of each mAb were injected two days before SFV administration; 100 µg on SFV treatments days and three days after the last SFV administration. A single dose of 300 µg anti-CD25-Rat IgG (PC61, in-house) or 200 µg anti-CD25-mIgG2a (33) was administered two days before SFV administration. Depletions were verified by peripheral blood flow cytometry staining. 100 µg p60 peptide (34) were administered i.p. daily for 10 days, starting two days before SFV administration. Tumor area was measured twice weekly and calculated as the product of orthogonal diameters.

Construction of SFV-derived vectors; mRNA quantitative analysis; Western Blotting: Tissue Processing and Flow cytometry; and Software and statistical analyses are detailed in Supplementary material and methods.

RESULTS

Characterization of SFV-derived vectors encoding sFLt3L and XCL1

Non-replicative SFV vectors were constructed by replacing the viral structural proteins with the mouse sequences of XCL1 or sFlt3L, generating vectors SFV-XCL1 and SFV-sFlt3L, respectively (Fig. 1A). An SFV vector expressing β-galactosidase encoded by LacZ gene (SFV-LacZ) was used for control purposes. An SFV vector encoding both XCL1 and sFlt3L as a single ORF was made by placing a 2A cis-protease sequence to permit post-translational efficient proteolytic separation of both transgene products. A furin cleavage site was also inserted to eliminate the remaining 2A target sequence from XCL1. Three cell lines were infected in culture with the different SFV vectors and quantitative RT-PCR detected strong transcription of the transgenes (Fig. 1B). Moreover, gene expression was readily detected in subcutaneous MC38-derived tumors excised 24h post-intratumoral injection of the corresponding SFV vectors (Fig. 1C). Of note, both *in vitro* and *in vivo*, the vector expressing the two transgenes showed comparatively lower quantities of each transgene mRNA as compared to single-gene SFV vectors, indicating less efficient expression in the double-transgene vector. Translation was confirmed by analyzing tissue culture cell-lysates of 24h-infected BHK cells by Western Blot (Fig. 1D). The differences in the sizes of the detected proteins encoded by the single-transgene and double-transgene vectors are due to the presence of a C-terminal myc tag from the XCL1 parental expression plasmid. Due to the cloning strategy used, the tag is present in the C-terminus of the XCL1 protein from SFV-XCL1 and from the sFlt3L protein from SFV-XF, thus slightly modifying their detected molecular weights in the Western Blot analysis.

Next, we examined the functionality of the expressed transgenes (Fig. 1E). For this purpose, we analyzed the chemotactic activity of XCL1 from tissue culture supernatants of SFV-infected BHK cells on iCD103 DCs derived in culture from bone marrow precursors as previously described (30) (Fig. 1F). sFlt3L bioactivity was assessed by studying the effect of infected BHK culture supernatants to

promote the differentiation of bone marrow cell suspensions into conventional and plasmacytoid DCs (cDCs and pDCs) (Fig. 1G). In both instances, transgene products appeared to be fully functional.

Antitumor activity of SFV vectors encoding sFlt3L and/or XCL1

To study the antitumor effects of the constructed SFV vectors, a single injection of 10^8 viral particles (VPs) was given into day 8 established MC38 subcutaneous tumors (Fig. 2A). A certain degree of tumor growth retardation was observed with all sFlt3L-containing SFV vectors, but it was more prominent with the vector encoding both XCL1 and sFLt3L (SFV-XF). To enhance antitumor effects, three doses of vectors were given every two days starting at day 8 after tumor cell inoculation. Again, MC38 tumors were more efficiently delayed in their growth by the SFV-XF vector (Supp. Fig. 1A). In a series of experiments represented in Figures 2 B and C, evident tumor growth delays were achieved by repeated intratumoral administration of SFV-XF into established MC38 (Fig. 2B) and B16-OVA (Fig. 2C) tumors. This treatment resulted in survival prolongation in both models but seldom in tumor eradication. Treatment of subcutaneous B16F10-derived melanomas, Panc02-derived pancreatic carcinomas and CT26-derived colon carcinomas with three viral doses also showed the therapeutic effects of SFV-XF (Supp. Fig. 1B-D) over saline control and SFV-LacZ, albeit SFV-LacZ showed some degree of activity on some of the transplanted tumor models.

Given the clinical success of immunomodulatory monoclonal antibodies (mAbs), we explored whether local SFV therapeutic activity could be potentiated by its combination with systemic antagonist anti-PD-1 or anti-CTLA-4 mAb, as well as with agonist anti-CD137 mAbs. As shown in Fig. 3, while the anti-CD137 mAb was able to delay tumor growth in both models, anti-PD-1 was almost ineffective against either model (Fig. 3A and B). Anti-CTLA-4 monotherapy was effective against MC38 tumors but not against B16-OVA tumors. In combination with a single dose of SFV-XF, systemic anti-CD137 mAb enhanced efficacy against MC38 and B16OVA tumors, while systemic anti-

PD-1 enhanced activity only against B16OVA. Anti-CTLA-4 mAb effects were potentiated both by SFV-XF and SFV-LacZ against B16OVA (Figure 3).

Antitumor activity of SFV-XF was dependent on CD8 T cells but markedly enhanced by CD4 T-cell depletion

To study the cellular requirements for the activity of SFV-XF, selective depletion of T-cell subsets and NK1.1[+] NK and NKT cells were performed prior to treatment in MC38 tumor-bearing mice. As shown in Fig. 4A, depletion of CD8β cells abolished therapeutic activity whilst CD4 and NK1.1 depletion enhanced the therapeutic effects, leading to extended survival. This result indicates that the antitumor effect mediated by SFV-XF is mainly mediated by CD8^{+} T cells.

One interpretation of the enhanced antitumor activity following CD4 depletion is the ensuing elimination of CD4^{+} Tregs. However, pre-depletion of Tregs with an anti-CD25 mAb (35) or inhibition of Foxp3 with an antagonist peptide (34) did not enhance therapeutic effects (Supp. Fig. 2A). In contrast, CD4 T-cell depletion gave rise to 4 out of 5 mice eradicating their tumors upon intratumoral treatment with SFV-XF in this experiment. Moreover, when an anti-CD25 mouse IgG2a that optimally depletes intratumoral Tregs was used, it did not show therapeutic synergy with SFV-XF against MC38 tumors, even though it exerted strong activity by itself (suppl. fig 2B). Completeness of depletions in peripheral blood was checked by flow cytometry (Suppl. fig 2C).

Since Treg depletion did not appear to be the mechanistic explanation, we focused on the effector CD4 T-cell cytokine production profile. In experiments shown in supplementary figure 3, B16-OVA bearing mice were adoptively transferred with TCR-transgenic OVA-reactive OT-II cells on day 7 and one day later intratumorally treated with SFV-XF, SFV-LacZ or saline. Intracellular cytokine staining for IFNγ, IL-10 and IL-17 in endogenous (suppl. fig 3A) and adoptively transferred (suppl. fig 3B) CD4 T cells from TDLNs was interrogated following an ex-vivo 4-hour stimulation with PMA+ION. Both in

endogenous CD4 and OT-II T cells a decrease of IFNγ and IL-17 producing fractions was observed while there were increases of IL-10 in the OT-II cells. These data suggest hampered Th1 differentiation upon SFV vector treatment potentially leading to deleterious effects of non-Treg CD4 subsets.

In mice bilaterally engrafted with MC38 tumors, SFV-XF treatment in the context of CD4 T-cell, but not NK1.1 depletion, undoubtedly delayed the growth of the concomitant distant non-injected tumors (Fig 4B and C). Similar effects on the contralateral tumors were observed in the B16OVA model (suppl fig 4 A and B). SFV-XF as a single agent did not have therapeutic effects on distant tumors, even though a trend for delay of tumor growth was observed in some of the experiments (Fig. 4C and suppl fig 4B).

SFV-XF increases effector T-cell infiltration of the B16OVA tumor microenvironment.

Upon treatment with SFV-XF of B16-OVA-derived tumors, there was an increase of CD4 and CD8 T-cell content in the tumor microenvironment detectable in directly treated tumors but also in concomitant non-directly injected contralateral lesions (Fig 5A). In these B16-OVA tumors, we observed a rapid increase in the number of H-2K^b-tetramer-positive CD8 T cells recognizing the OVA-specific SIINFEKL epitope contingent on SFV-XF treatment (Fig. 5B). However, these effects in the tumor microenvironment were not found under similar conditions of treatment in MC38 derived tumors (suppl fig 5A and B), indicating model-inherent differences in spite of the fact that both models respond to treatment.

Interestingly, in bilaterally engrafted B16OVA-bearing mice in which CD4 depletion was induced 48 h prior to intratumoral SFV vector injection to one of the tumors there were more prominent bilateral increases in the content of antigen-specific CD8 cells among tumor-infiltrating T cells (fig 5B). CD4 depletion also markedly increased bilaterally the percentage of proliferating Ki67+ CD8 T cells (fig

5C). In the MC38 bilateral model, intratumoral percentage of proliferating Ki67+ CD8 T cells also increased in response to CD4-depletion and SFV-XF (suppl. fig 5C). These results indicate increases in tumor-reactive CTLs consistent with the results of CD8 depletion experiments and support that CD4-depletion further potentiates tumor-specific CD8 T cells in the context of intratumoral SFV-XF treatment. In light of the effects of SFV-XF in combination with immunostimulatory monoclonal antibodies in B16OVA and MC38 bilaterally engrafted mice, we analyzed the percentage of expression of CD137, CTLA-4, PD-1 and LAG-3 on CD8 and non-Treg CD4 tumor-infiltrating T cells following intratumoral treatment with SFV vectors. In the case of CD8 T cells, expression was also monitored upon concomitant CD4-depletion. As shown in supplementary figure 6A, CD8 T cells expressing CTLA-4, PD-1 and LAG-3 increased in the treated tumor with moderate increases of CD137 expression. Percentages of cells expressing these checkpoints were further increased by CD4 co-depletion. Percentages of PD-1, CTLA-4 and LAG-3 expressing CD4 T cells were also increased by SFV-XF treatment (suppl. Fig 6B). Again, such changes were not observed in MC38 bearing mice (suppl fig 6C and D). FACS-Gating strategies for tumor-infiltrating T-cell studies are shown in supplementary figure 7A. At least in the B16OVA model, additive effects of systemic immunostimulatory monoclonal antibodies with intratumoral SFV-XF could be explained in part by enhanced expression of the co-inhibitory or costimulatory T-cell targets.

SFV-XF therapeutic activity is contingent on BATF3-dependent DC integrity and causes cDC1 accumulation in tumor-draining lymph nodes (TDLNs)

Experiments were performed in mice deficient in BATF3, which are virtually devoid of cDC1s (8). In these animals, the antitumor effects of SFV-XF seen in wild type (WT) control mice were completely lost (Fig. 6A, B). The integrity of the type-I interferon (IFN-I) system is required for the function of BATF3-dependent DCs (36) and for CD8 immunity (37). As seen in Figure 6A, efficacy was also lost, when treatment was given to *Ifnar*$^{-/-}$ mice. However, tumor growth delay was preserved to some

degree in STING KO mice, indicating at least partial independence of our therapy of the cGAS-STING pathway.

Given the activity of the SFV-encoded transgenes, we expected tumors to become infiltrated by cDC1s, a feature reported to correlate with better prognosis in human cancer (38,39). In B16OVA tumors increases not only in cDC1 but also in cDC2 were substantiated in terms of cells per mg of tissue (figure 7A). However, as seen in Fig. 7B, in MC38-derived tumors dendritic cell infiltrates did not significantly change following three intratumoral doses of SFV-XF over control or SFV-LacZ. In contrast, harvested TDLNs from SFV-XF-treated MC38 tumors showed marked increases in absolute numbers of both migratory (CD11c$^+$IAb^{hi}CD103$^+$CD11b$^-$) and resident (CD11c^{hi}IAb$^+$CD8α$^+$CD11b$^-$) cDC1 cells (Fig. 7C). In addition, there was a detectable increase in CD11b$^+$ cDC2 cells (Fig. 7B). FACS gating strategies for analysis are shown in supplementary Fig. 7B and C.

In conclusion, dependency on BATF3 and the increase of cross-presenting DCs in TDLNs are consistent with the immunotherapeutic activity of XCL1 and sFlt3L as SFV-encoded transgenes.

DISCUSSION

In this study, SFV vectors engineered to increase cross-priming of tumor antigens were tested following intratumoral injection. Although all SFV constructions encoding sFlt3L delayed tumor growth, the combination of the chemokine XCL1 and sFlt3L showed more marked antitumor effects on five different transplantable mouse models. Bioactivity of both transgenes was confirmed using the supernatant of infected cells in culture.

Intratumoral injection of viral vectors including HSV (40), measles virus (41), Vaccinia virus (42), VSV (43) and reovirus (44) is gaining momentum in tumor immunotherapy (6). Their intratumoral administration frequently leads to meaningful therapeutic effects, particularly when combined with anti-CTLA-4 or anti-PD-1 checkpoint inhibitors (5,45). In the case of alphavirus vectors, an SFV virus encoding IL-12 exerts potent antitumor effects dependent on CD8 T-cell antitumor immunity (22). SFV-XF was therapeutically less potent than an SFV vector encoding IL-12, although it has the advantage that IL-12 uncontrolled production might have safety problems, as reported in human patients systemically given the recombinant protein (46). In this regard, Flt3L recombinant protein is reportedly safe in humans following repeated subcutaneous administration (47).

The original objective of the SFV-XF vector was to enhance tumor antigen cross-presentation by means of attracting and differentiating cDC1s and thereby enhancing CD8 T-cell cross-priming. Indeed, the SFV-XF encoded transgenes exert these effects on cells in culture. We had previously shown two important features of SFV-based local immunotherapy: (i) it provides abundant viral RNA that enhances TLR3 and helicase-dependent innate signals (28), and (ii) it enhances local IFNα/β through these mechanisms (28). These two effects, in conjunction with a more prominent cDC1 infiltrate and function should prime and sustain cellular antitumor immunity. In this context, it was surprising that SFV-XF showed a rather modest anti-tumor activity, although most tumors were delayed in their growth after treatment. Additive effects were observed upon combination with anti-

15

CD137, anti-PD1 and anti-CTLA-4 immunostimulatory monoclonal antibodies that probably involve some degree of induced expression of their lymphocyte targets on tumor-reactive T cells. Of note, intratumoral SFV-IL12 is reportedly highly synergistic with these immunomodulatory antibodies (24,25).

Experiments upon depletion of CD8 T cells were consistent with a necessary involvement of CTLs in the antitumor effects. Surprisingly, CD4 T-cell depletion and NK/NKT depletion gave rise to enhanced therapeutic activity. Furthermore we have used a mIgG2a version of the anti-CD25 mAb to ensure intratumoral Treg depletion and this treatment did not potentiate SFV-XF antitumor activity, although this antibody had a high antitumor effect by itself (33). Having ruled out a simple explanation based on the elimination of Tregs by CD25 depletion and Foxp3 inhibition, our next hypothesis was that lymphopenia secondary to CD4 depletion augmented the availability of homeostatic cytokines such as IL-7 or IL-15 for CD8 T cells. However, we were unable to detect increased circulating levels of these cytokines following depletion. It is of note that the $CD4^+Foxp3^-$ and $CD4^+Foxp3^+$ infiltrate increases 48 hours following SFV-XF intratumoral administration (Fig. 6A), potentially affecting locally the therapeutic actions of the recombinant virus.

Next we examined if SFV-XF intratumoral treatment altered the cytokine production profile of effector CD4 T cells in tumor draining lymph nodes. These experiments showed an SFV-induced reduction in the number of CD4 T cells able to produce IFNγ and an increase of those producing IL-10 (Suppl fig. 3). In this context, CD4 depletion is likely to be counteracting this deleterious effect for anti-tumor activity. Observations on tumor-infiltrating CD8 T cells in the B16OVA tumor model are consistent with a relief of an inhibitory mechanism by CD4 depletion.

The mechanistic interplay of NK and NKT cells to dampen the efficacy of SFV-XF remains to be elucidated, although some reports suggest an inhibitory activity of NK cells on recently activated CD8 T-cell blasts (48,49).

SFV-XF intratumoral treatment in the bilateral B16OVA tumor model gave rise to marked increases in activated and tumor specific CD8 T cells taking place both in the directly treated tumor and in the non-injected contralateral side. Indeed, such increases were markedly enhanced by CD4 concomitant depletion. In spite of therapeutic activity, such tumor microenvironment observations were not reproduced in the MC38 model, a fact that could reflect intrinsic differences between the models or differences in the time course of T-cell infiltration changes.

In keeping with the function of the XCL1 and sFlt3L transgenes, antitumor effects were contingent on BATF3-dependent DCs. Notably, we observe an increase in such DCs in the tumor microenvironment following SFV-XF intratumoral administration to B16OVA-derived tumors. Increased numbers of DC included not only cDC1 but also cDC2. It remains to be seen if such increased intratumoral DC subsets are properly performing tumor-antigen presentation. Intratumoral DC were not increased in the MC38 model but there were marked increases found in TDLNs that were minimally seen in distant lymphoid organs. These were also seen, to a much lesser extent, in TDLNs from non-treated distant subcutaneous tumors obtained in the same way, probably due to an accumulation of circulating Flt3L after repeated SFV-XF administrations. Such increased cDC1 cells belonged to both resident and migratory phenotypes, suggesting that perhaps part of these cDC1 cells seen in TDLNs might have been in the tumor tissue at some earlier time points. In fact, innate effects of SFV RNA may induce maturation and rapid migration of cDC1s out of tumor tissue to TDLNs, thus explaining that cDC1 numbers are not increased in the TME of MC38 tumors. Further enhancement of cDC1 content in the tumor microenvironment warrants future research, for instance using other chemokines known to attract this DC subset, such as CCL4 (50). However, in two recent articles, XCL1 and FLT3L as produced by NK cells were found to dictate cDC1 presence in the tumor microenvironment (18,51).

The striking therapeutic effect of SFV-XF combination with CD4 depletion which led to a certain degree of efficacy against distant tumors (Fig. 4B and Supp. Fig. 4B) is difficult to translate into the

clinic, since CD4 depletion is highly immunosuppressive and in practice could only be induced transiently. CD4 T-cell immunity is complex and encompasses both antitumor and protumor activities. Transplanted tumors in mice, as opposed to human malignancies, grow fast in the two weeks following tumor cell inoculation and the mechanism of action of SFV-XF, relying on cross-priming, might take longer to properly begin. In fact, DC numbers kept increasing in TDLNs from treated mice over time. Little is known about the functional interplay of CD4 T cells and cDC1s, and our results call for an in-depth study.

All in all, our results indicate interesting immunobiological effects of SFV-mediated XCL1 and sFlt3L local gene transfer into tumors that might find suitable combination partners for effective cancer immunotherapy. The strategy is of much interest due to its effects on antigen-presenting cells specialized in CD8 T-cell cross-priming.

REFERENCES

1.   Melero I, Grimaldi AM, Perez-Gracia JL, Ascierto PA. Clinical development of immunostimulatory monoclonal antibodies and opportunities for combination. Clin Cancer Res. 2013;19:997–1008.

2.   Aznar MA, Tinari N, Rullán AJ, Sánchez-Paulete AR, Rodriguez-Ruiz ME, Melero I. Intratumoral Delivery of Immunotherapy—Act Locally, Think Globally. J Immunol. 2017;198:31–9.

3.   Corrales L, Glickman LH, McWhirter SM, Kanne DB, Sivick KE, Katibah GE, et al. Direct Activation of STING in the Tumor Microenvironment Leads to Potent and Systemic Tumor Regression and Immunity. Cell Rep. 2015/05/12. The Authors; 2015;11:1018–30.

4.   Rakoff-Nahoum S, Medzhitov R. Toll-like receptors and cancer. Nat Rev Cancer. 2009;9:57–63.

5.   Ribas A, Dummer R, Puzanov I, VanderWalde A, Andtbacka RHI, Michielin O, et al. Oncolytic Virotherapy Promotes Intratumoral T Cell Infiltration and Improves Anti-PD-1 Immunotherapy. Cell. 2017;170:1109–1119.e10.

6.   Lichty BD, Breitbach CJ, Stojdl DF, Bell JC. Going viral with cancer immunotherapy. Nat Rev Cancer. 2014/07/06. Nature Publishing Group; 2014;14:559–67.

7.   Sánchez-Paulete AR, Teijeira Á, Cueto FJ, Garasa S, Pérez-Gracia JL, Sánchez-Arráez Á, et al. Antigen Cross-Presentation and T-Cell Cross-Priming In Cancer Immunology And Immunotherapy. Ann Oncol. 2017;28:xii44-xii55.

8.   Hildner K, Edelson BT, Purtha WE, Diamond M, Matsushita H, Kohyama M, et al. Batf3 Deficiency Reveals a Critical Role for CD8 + Dendritic Cells in Cytotoxic T Cell Immunity. Science (80-). 2008;322:1097–100.

9.   Grajales-Reyes GE, Iwata A, Albring J, Wu X, Tussiwand R, KC W, et al. Batf3 maintains autoactivation of Irf8 for commitment of a CD8α+ conventional DC clonogenic progenitor. Nat Immunol. 2015;16:708–17.

10.   Sánchez-Paulete AR, Cueto FJ, Martínez-López M, Labiano S, Morales-Kastresana A, Rodríguez-Ruiz ME, et al. Cancer Immunotherapy with Immunomodulatory Anti-CD137 and Anti-PD-1 Monoclonal Antibodies Requires BATF3-Dependent Dendritic Cells. Cancer Discov. 2016;6:71–9.

11.   Gerner MY, Casey KA, Kastenmuller W, Germain RN. Dendritic cell and antigen dispersal landscapes regulate T cell immunity. J Exp Med. 2017;214:jem.20170335.

12.   Edelson BT, KC W, Juang R, Kohyama M, Benoit LA, Klekotka PA, et al. Peripheral CD103 [+] dendritic cells form a unified subset developmentally related to CD8α [+] conventional dendritic cells. J Exp Med. 2010;207:823–36.

13.   Salmon H, Idoyaga J, Rahman A, Leboeuf M, Remark R, Jordan S, et al. Expansion and Activation of CD103+ Dendritic Cell Progenitors at the Tumor Site Enhances Tumor Responses to Therapeutic PD-L1 and BRAF Inhibition. Immunity. 2016/04/21. 2016;44:924–38.

14.   Roberts EW, Broz ML, Binnewies M, Headley MB, Nelson AE, Wolf DM, et al. Critical Role for CD103+/CD141+ Dendritic Cells Bearing CCR7 for Tumor Antigen Trafficking and Priming of T Cell Immunity in Melanoma. Cancer Cell. Elsevier Inc.; 2016;30:324–36.

15.   Maraskovsky E. Dramatic increase in the numbers of functionally mature dendritic cells in Flt3 ligand-treated mice: multiple dendritic cell subpopulations identified. J Exp Med.

1996;184:1953–62.

16.   Yamazaki C, Sugiyama M, Ohta T, Hemmi H, Hamada E, Sasaki I, et al. Critical Roles of a Dendritic Cell Subset Expressing a Chemokine Receptor, XCR1. J Immunol. 2013;190:6071–82.

17.   Dorner BG, Dorner MB, Zhou X, Opitz C, Mora A, Güttler S, et al. Selective Expression of the Chemokine Receptor XCR1 on Cross-presenting Dendritic Cells Determines Cooperation with CD8+ T Cells. Immunity. 2009;31:823–33.

18.   Böttcher JP, Bonavita E, Chakravarty P, Blees H, Cabeza-Cabrerizo M, Sammicheli S, et al. NK Cells Stimulate Recruitment of cDC1 into the Tumor Microenvironment Promoting Cancer Immune Control. Cell. 2018;0:1–16.

19.   Poulin LF, Salio M, Griessinger E, Anjos-Afonso F, Craciun L, Chen J-L, et al. Characterization of human DNGR-1 + BDCA3 + leukocytes as putative equivalents of mouse CD8α + dendritic cells. J Exp Med. 2010;207:1261–71.

20.   Ying H, Zaks TZ, Wang RF, Irvine KR, Kammula US, Marincola FM, et al. Cancer therapy using a self-replicating RNA vaccine. Nat Med. 1999;5:823–7.

21.   Diebold SS, Schulz O, Alexopoulou L, Leitner WW, Flavell RA, Reis e Sousa C. Role of TLR3 in the immunogenicity of replicon plasmid-based vaccines. Gene Ther. 2009;16:359–66.

22.   Rodriguez-Madoz JR, Prieto J, Smerdou C. Semliki forest virus vectors engineered to express higher IL-12 levels induce efficient elimination of murine colon adenocarcinomas. Mol Ther. 2005;12:153–63.

23.   Rodriguez-Madoz JR, Liu KH, Quetglas JI, Ruiz-Guillen M, Otano I, Crettaz J, et al. Semliki Forest Virus Expressing Interleukin-12 Induces Antiviral and Antitumoral Responses in Woodchucks with Chronic Viral Hepatitis and Hepatocellular Carcinoma. J Virol. 2009;83:12266–78.

24.   Quetglas JI, Labiano S, Aznar MA, Bolanos E, Azpilikueta A, Rodriguez I, et al. Virotherapy with a Semliki Forest Virus-Based Vector Encoding IL12 Synergizes with PD-1/PD-L1 Blockade. Cancer Immunol Res. 2015;3:449–54.

25.   Quetglas JI, Dubrot J, Bezunartea J, Sanmamed MF, Hervas-Stubbs S, Smerdou C, et al. Immunotherapeutic Synergy Between Anti-CD137 mAb and Intratumoral Administration of a Cytopathic Semliki Forest Virus Encoding IL-12. Mol Ther. 2012;20:1664–75.

26.   Curran MA, Montalvo W, Yagita H, Allison JP. PD-1 and CTLA-4 combination blockade expands infiltrating T cells and reduces regulatory T and myeloid cells within B16 melanoma tumors. Proc Natl Acad Sci. National Acad Sciences; 2010;107:4275–80.

27.   Huang H, Li F, Gordon JR, Xiang J. Synergistic enhancement of antitumor immunity with adoptively transferred tumor-specific CD4+and CD8+T cells and intratumoral lymphotactin transgene expression. Cancer Res. 2002;62:2043–51.

28.   Melero I, Quetglas JI, Reboredo M, Dubrot J, Rodriguez-Madoz JR, Mancheño U, et al. Strict requirement for vector-induced type I interferon in efficacious antitumor responses to virally encoded IL12. Cancer Res. 2015;75:497–507.

29.   Mazzolini G, Narvaiza I, Martinez-Cruz LA, Arina A, Barajas M, Galofré JC, et al. Pancreatic cancer escape variants that evade immunogene therapy through loss of sensitivity to IFNgamma-induced apoptosis. Gene Ther. 2003;10:1067–78.

30.   Mayer CT, Ghorbani P, Nandan A, Dudek M, Arnold-Schrauf C, Hesse C, et al. Selective and efficient generation of functional Batf3-dependent CD103+ dendritic cells from mouse bone

marrow. Blood. 2014;124:3081–91.

31.   Sauer JD, Sotelo-Troha K, Von Moltke J, Monroe KM, Rae CS, Brubaker SW, et al. The N-ethyl-N-nitrosourea-induced Goldenticket mouse mutant reveals an essential function of sting in the in vivo interferon response to Listeria monocytogenes and cyclic dinucleotides. Infect Immun. American Society for Microbiology; 2011;79:688–94.

32.   Schilte C, Couderc T, Chretien F, Sourisseau M, Gangneux N, Guivel-Benhassine F, et al. Type I IFN controls chikungunya virus via its action on nonhematopoietic cells. J Exp Med. The Rockefeller University Press; 2010;207:429–42.

33.   Arce Vargas F, Furness AJS, Solomon I, Joshi K, Mekkaoui L, Lesko MH, et al. Fc-Optimized Anti-CD25 Depletes Tumor-Infiltrating Regulatory T Cells and Synergizes with PD-1 Blockade to Eradicate Established Tumors. Immunity. 2017;46:577–86.

34.   Casares N, Rudilla F, Arribillaga L, Llopiz D, Riezu-Boj JI, Lozano T, et al. A Peptide Inhibitor of FOXP3 Impairs Regulatory T Cell Activity and Improves Vaccine Efficacy in Mice. J Immunol. 2010;185:5150–9.

35.   Casares N, Arribillaga L, Sarobe P, Dotor J, Lopez-Diaz de Cerio A, Melero I, et al. CD4+/CD25+ regulatory cells inhibit activation of tumor-primed CD4+ T cells with IFN-gamma-dependent antiangiogenic activity, as well as long-lasting tumor immunity elicited by peptide vaccination. J Immunol. 2003;171:5931–9.

36.   Fuertes MB, Kacha AK, Kline J, Woo S-R, Kranz DM, Murphy KM, et al. Host type I IFN signals are required for antitumor CD8 [+] T cell responses through CD8α [+] dendritic cells. J Exp Med. 2011;208:2005–16.

37.   Diamond MS, Kinder M, Matsushita H, Mashayekhi M, Dunn GP, Archambault JM, et al. Type I interferon is selectively required by dendritic cells for immune rejection of tumors. J Exp Med. 2011;208:1989–2003.

38.   Broz ML, Binnewies M, Boldajipour B, Nelson AE, Pollack JL, Erle DJ, et al. Dissecting the Tumor Myeloid Compartment Reveals Rare Activating Antigen-Presenting Cells Critical for T Cell Immunity. Cancer Cell. Elsevier Inc.; 2014;26:638–52.

39.   Spranger S, Dai D, Horton B, Gajewski TF. Tumor-Residing Batf3 Dendritic Cells Are Required for Effector T Cell Trafficking and Adoptive T Cell Therapy. Cancer Cell. Elsevier Inc.; 2017;31:711–723.e4.

40.   Moesta AK, Cooke K, Piasecki J, Mitchell P, Rottman JB, Fitzgerald K, et al. Local Delivery of OncoVEX mGM-CSF Generates Systemic Antitumor Immune Responses Enhanced by Cytotoxic T-Lymphocyte–Associated Protein Blockade. Clin Cancer Res. 2017;23:6190–202.

41.   Veinalde R, Grossardt C, Hartmann L, Bourgeois-Daigneault M-C, Bell JC, Jäger D, et al. Oncolytic measles virus encoding interleukin-12 mediates potent antitumor effects through T cell activation. Oncoimmunology. 2017;6:e1285992.

42.   Dai P, Wang W, Yang N, Serna-Tamayo C, Ricca JM, Zamarin D, et al. Intratumoral delivery of inactivated modified vaccinia virus Ankara (iMVA) induces systemic antitumor immunity via STING and Batf3-dependent dendritic cells. Sci Immunol. Science Immunology; 2017;2:eaal1713.

43.   Diaz RM, Galivo F, Kottke T, Wongthida P, Qiao J, Thompson J, et al. Oncolytic immunovirotherapy for melanoma using vesicular stomatitis virus. Cancer Res. 2007;67:2840–8.

44. Rajani K, Parrish C, Kottke T, Thompson J, Zaidi S, Ilett L, et al. Combination therapy with reovirus and Anti-PD-1 blockade controls tumor growth through innate and adaptive immune responses. Mol Ther. 2016;24:166–74.

45. Puzanov I, Milhem MM, Minor D, Hamid O, Li A, Chen L, et al. Talimogene laherparepvec in combination with ipilimumab in previously untreated, unresectable stage IIIB-IV melanoma. J Clin Oncol. 2016;34:2619–26.

46. Atkins MB, Robertson MJ, Gordon M, Lotze MT, DeCoste M, DuBois JS, et al. Phase I evaluation of intravenous recombinant human interleukin 12 in patients with advanced malignancies. Clin Cancer Res. 1997;3:409–17.

47. Breton G, Lee J, Zhou YJ, Schreiber JJ, Keler T, Puhr S, et al. Circulating precursors of human CD1c [+] and CD141 [+] dendritic cells. J Exp Med. 2015;212:401–13.

48. Crouse J, Bedenikovic G, Wiesel M, Ibberson M, Xenarios I, VonLaer D, et al. Type I Interferons Protect T Cells against NK Cell Attack Mediated by the Activating Receptor NCR1. Immunity. 2014;40:961–73.

49. Xu HC, Grusdat M, Pandyra AA, Polz R, Huang J, Sharma P, et al. Type I Interferon Protects Antiviral CD8+T Cells from NK Cell Cytotoxicity. Immunity. 2014;40:949–60.

50. Spranger S, Bao R, Gajewski TF. Melanoma-intrinsic β-catenin signalling prevents anti-tumour immunity. Nature. 2015;523:231–5.

51. Barry KC, Hsu J, Broz ML, Cueto FJ, Binnewies M, Combes AJ, et al. A natural killer–dendritic cell axis defines checkpoint therapy–responsive tumor microenvironments. Nat Med. Springer US; 2018;

Figure 1. SFV-based vectors confer functional expression of XCL1 and/or Flt3L in infected cells

(A) XCL1 and/or soluble Flt3L (sFlt3L) cDNAs were cloned into the SFV vector backbone encoding SFV non-structural proteins (nsp 1-4). (B and D) BHK, MC38 and B16-OVA cell lines were infected in culture with SFV-derived vectors and transgene expression was assessed 24h later by quantitative RT-PCR (B) or Western Blot analysis with antibodies specific for the indicated proteins (D). Ct values were normalized for β-actin (βact) or SFV replicase (replicase). (C) MC38 subcutaneous tumors were established and intratumorally injected with 10^8 SFV viral particles when they reached an approximate size of 25 mm^2. Transgene expression was assessed 24h later by quantitative RT-PCR. (E) BHK cells were infected with SFV-derived vectors at a multiplicity of infection (MOI) of 10 and cell-free supernatants were collected 24h later and used for the indicated assays. (F) iCD103 cells were derived from bone marrow in 14-day cultures in the presence of sFlt3L and GM-CSF as described (30). For chemotaxis assays, 10^5 iCD103 cells were placed onto a 5-μm transwell membrane chambers and allowed to migrate towards infected BHK-supernatants for 4h. Total migrated cells in the lower chamber were quantified by flow cytometry. One representative experiment is shown out of three. (G) Bone marrow cell suspensions flushed out of mouse bones were differentiated *ex vivo* for nine days using infected BHK supernatant-conditioned media. On day 9, cultures were analyzed by flow cytometry. Conventional DCs (cDCs) were identified as CD11c$^+$CD11b$^+$ and plasmacytoid DCs (pDCs) as CD11c$^+$B220$^+$CD11b$^-$. One representative experiment is shown out of three. **p<0.01; ***p<0.001 (One-way ANOVA). (A)$_n$, polyA; furin, target sequence for furin protease; p2A, 2A autoprotease from foot and mouth disease virus.

Figure 2. Intratumoral injection of SFV-XF exerts antitumor effects against MC38 and B16-OVA subcutaneous tumors

(A and B) 5 x 10^5 MC38 cells were inoculated subcutaneously into the right flank of C57Bl/6 mice. (A) Mice received one intratumoral dose of 10^8 VPs of SFV-derived vectors on day 8 (indicated by the dotted line). Results represent mean tumor size evolution from one representative experiment with 6 mice per group of four experiments performed. (B) Mice received three intratumoral doses of 10^8 VPs of SFV-derived vectors on days 8, 10, and 12 (dotted lines). Data represent mean tumor size evolution over time (upper panel) from one representative experiment with six mice per group of three experiments performed as well as survival of the mice (Kaplan-Meier curves in lower panel) summarizing three pooled experiments. Fractions indicate surviving mice at the end of the experiment. (C) 5 x 10^5 B16-OVA cells were inoculated subcutaneously into the flank of C57Bl/6 mice. Mice received three intratumoral doses of 10^8 VPs of SFV-derived vectors on days 6, 8, and 10 (indicated by dotted lines). Mean tumor sizes over time (upper panel) from one representative experiment with seven mice per group of two experiments performed and survival of the mice (lower panel) from the two pooled experiments are represented. *p<0.05; **p<0.01; ***p<0.001.

Figure 3. Intratumoral treatment with SFV-XF shows additive therapeutic effects with anti-CD137, anti-PD-1 or anti-CTLA-4 immunomodulatory mAbs.

(A) 5 x 10^5 MC38 or (B) 5 x 10^5 B16-OVA cells were inoculated subcutaneously into the flank of C57Bl/6 mice. Mice received one intratumoral dose of 10^8 VPs of the indicated SFV vectors on day 7 (vertical dotted lines) and three intraperitoneal doses of anti-CD137, anti-PD-1 or antiCTLA-4 mAbs on days 7, 10, and 13 (vertical dashed lines). Mean tumor size evolutions over time are represented (n = 5-6 mice per group). Statistical comparisons between antibody treatment groups are presented on the right handside of the graphs. +p<0.1, *p<0.05; **p<0.01; ***p<0.001, ns: non significant.

Figure 4. CD8 T-cell depletion abrogates SFV-XF therapeutic effects, whereas CD4-T cell depletion markedly improves efficacy

(A) 5×10^5 MC38 cells were inoculated subcutaneously into the flank of C57Bl/6 mice. Three intratumoral doses of 10^8 VPs of SFV-XF were given on days 7, 9, and 11 (dotted lines). Results show mean tumor progression from one representative experiment of two performed (left panel) and survival summarizes two pooled experiments (right panel). Fractions indicate surviving tumor-free mice at the end of the experiment. (B,C) 5×10^5 and 3×10^5 MC38 cells, respectively, were inoculated into the right and left flanks of C57Bl/6 mice and the right flank tumor was treated as described in (A). Results represent mean fold increase in tumor growth over time. All mice received intraperitoneal injections of depleting antibodies and depletions were confirmed as described in Materials and Methods. $^+$p<0.1; *p<0.05; **p<0.01; ***p<0.001.

Figure 5. SFV-XF requires Batf3-dependent DCs and IFNAR for therapeutic activity

5×10^5 MC38 cells were inoculated subcutaneously into the flank of WT, *Batf3$^{-/-}$*, *Tmem173$^{-/-}$* (STING KO)*, or *Ifnar$^{-/-}$* mice with C57Bl/6 background. Three intratumoral doses of 10^8 VPs of SFV-derived vectors were given on days 7, 9, and 12 (dotted lines). Tumor sizes over time (A) and survival (B) from two pooled experiments are shown. Fractions in each graph indicate surviving mice. **p<0.01.

Figure 6. SFV-XF intratumoral treatment of B16OVA tumors bilaterally increases CD4 and CD8 T cell infiltration including tumor-reactive CTLs.

Bilateral B16OVA subcutaneous tumors were established by inoculation of 5×10^5 cells. CD4 depleting mAb were given on the days indicated by arrows and six groups of treatment were set up as indicated in the legend, injecting SFV-XF, SFV-LacZ or saline intratumorally on the marked days. (A) represents the number of CD45+, CD8+, CD4+FOX-P3- and Treg per mg of tumor tissue of the

indicated treatment groups in cell suspensions from local and contralateral (distant) tumors harvested on day 13. (B) represents number of CD8 T cells per mg of tumor stained by H-2K^b-SIINFEKL tetramer. (C) percentage of infiltrating CD8 T cells intracellularly stained for Ki-67.

Figure 7. Following SFV-XF treatment conventional DCs become enriched in the B16OVA tumor microenvironment and in tumor-draining LNs from MC38 tumors.

Schematic design of the experiments engrafting 5 x 10^5 B16OVA cells (A) or 5 x 10^5 MC38 cells (B). Established tumors received three intratumoral doses of 10^8 VPs of SFV-derived vectors or saline on the indicated days. cDC1 (CD103+) and cDC2 (CD11b+) are defined as shown in supplementary figure 7B. Three days after the last intratumoral administration , tumors and TDLNs were excised, digested, and single cell suspensions analyzed by flow cytometry. A and B graphs represent the number of cDC1 and cDC2 dendritic cells per mg of tumor (C) Absolute numbers of dendritic cells per MC38-draining LN are presented. Gating strategies for resident and migratory DCs are shown in Supplementary Figure 7C. $^+$p<0.1; *p<0.05; **p<0.01; ***p<0.001.
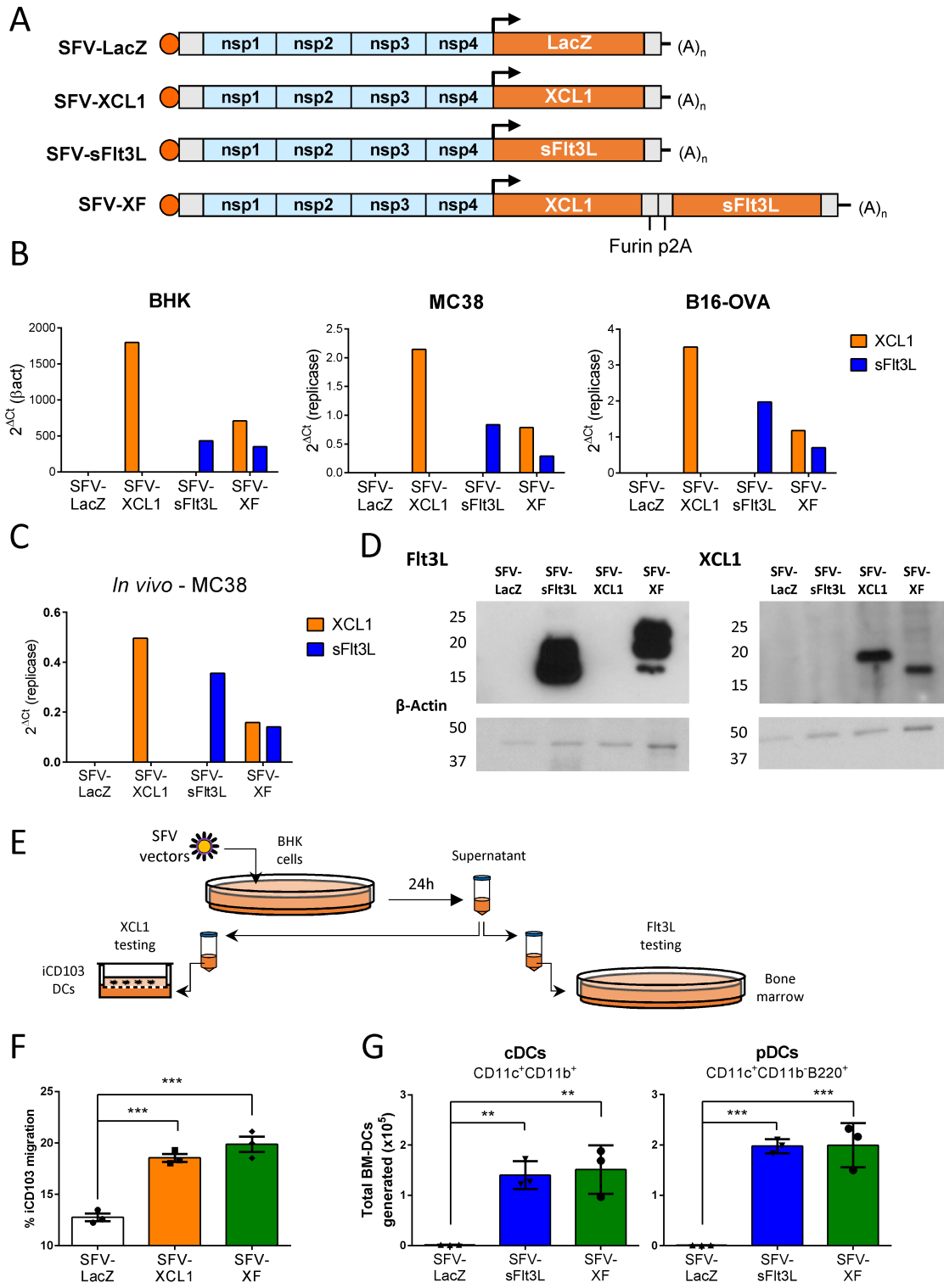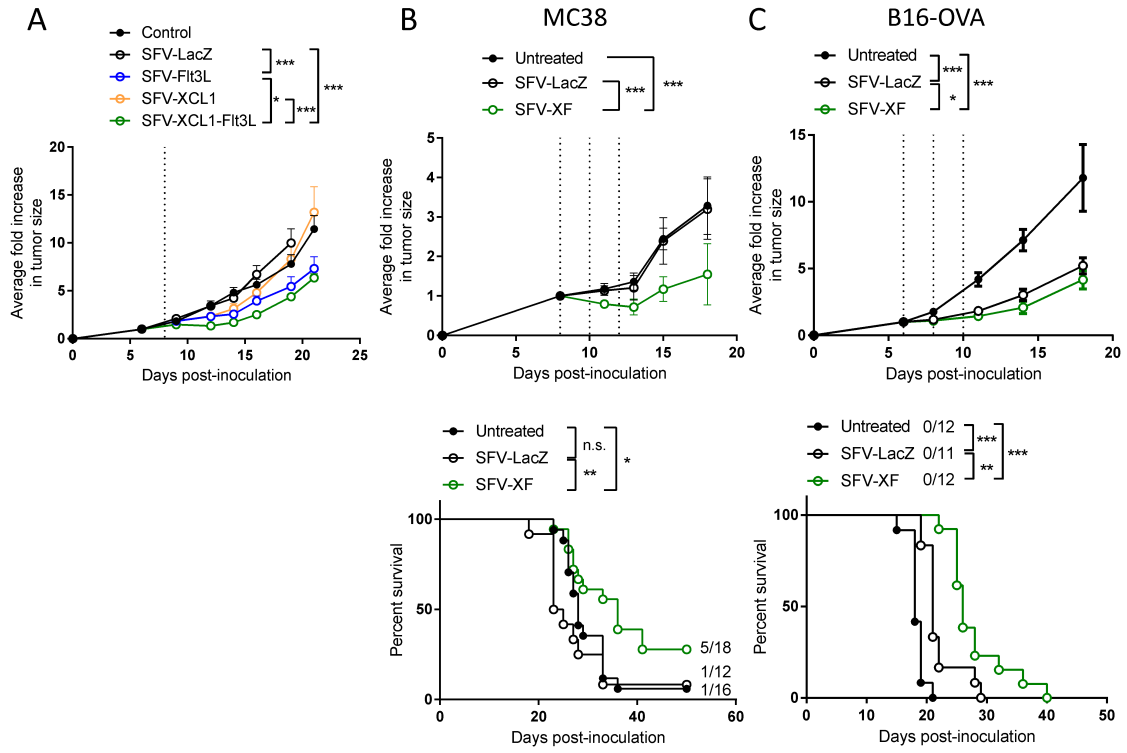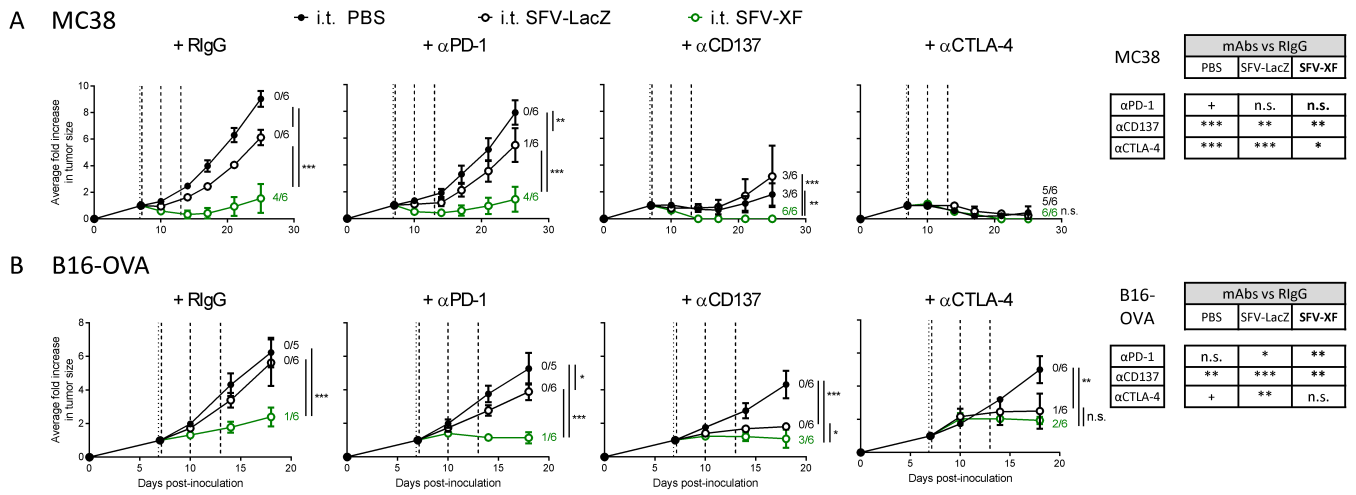
Figure 1

Figure 2

Figure 3

A   MC38

● i.t. PBS   ○ i.t. SFV-LacZ   ○ i.t. SFV-XF

MC38	mAbs vs RIgG		
	PBS	SFV-LacZ	**SFV-XF**
αPD-1	+	n.s.	**n.s.**
αCD137	***	**	**
αCTLA-4	***	***	*

B   B16-OVA

B16-OVA	mAbs vs RIgG		
	PBS	SFV-LacZ	**SFV-XF**
αPD-1	n.s.	*	**
αCD137	**	***	**
αCTLA-4	+	**	n.s.
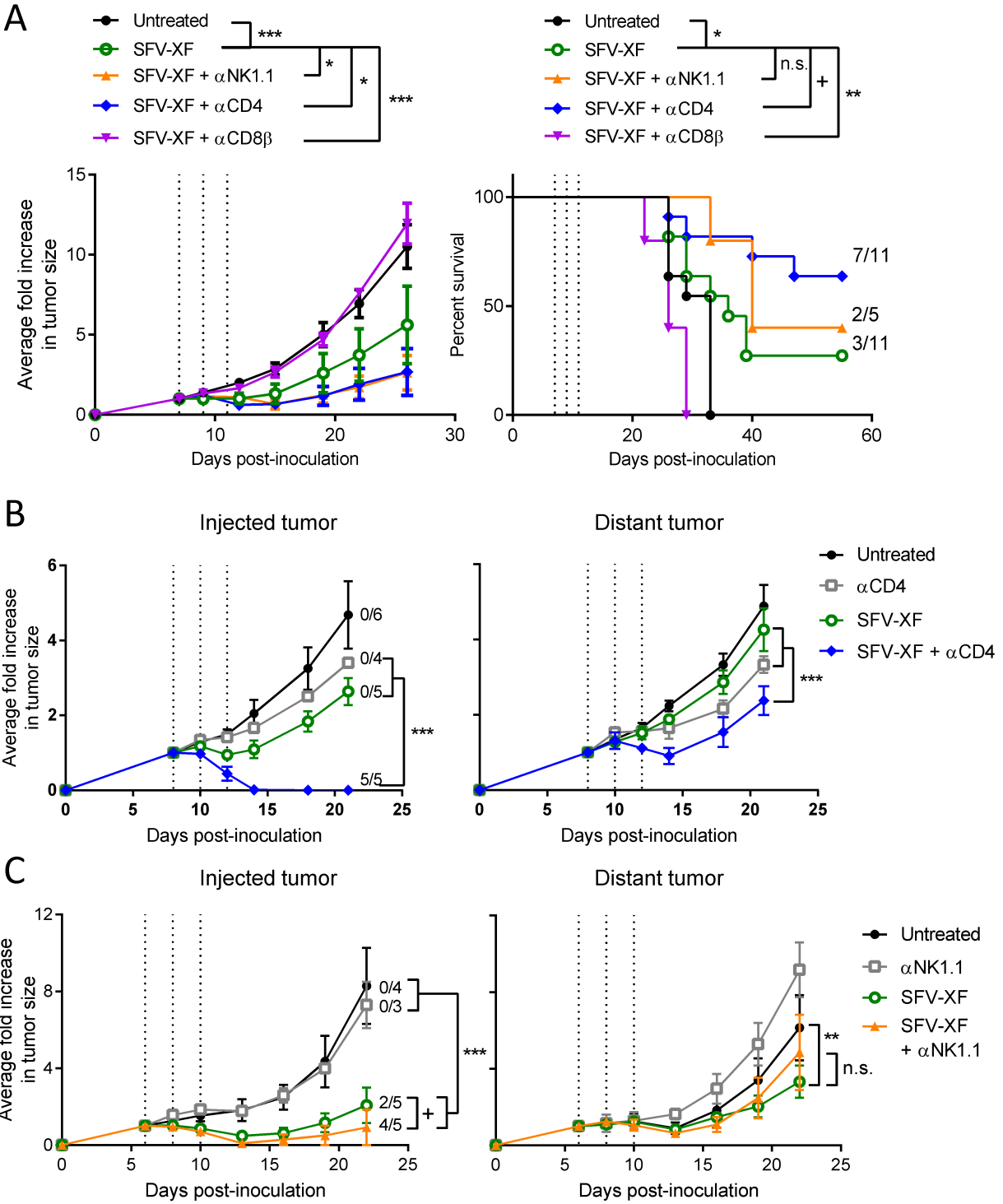
Figure 4

Figure 5

Figure 6

A
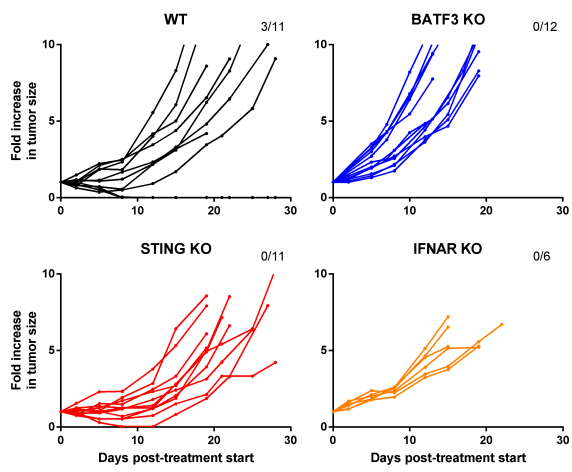
B
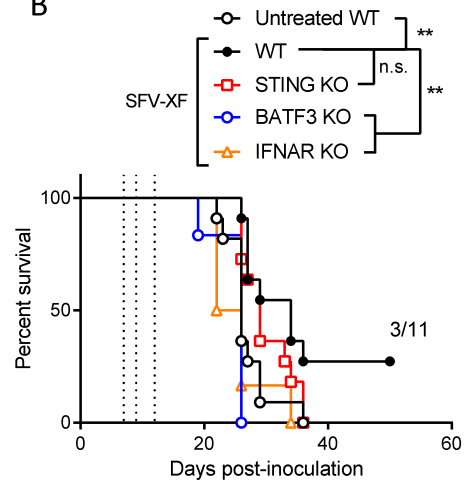
Figure 7
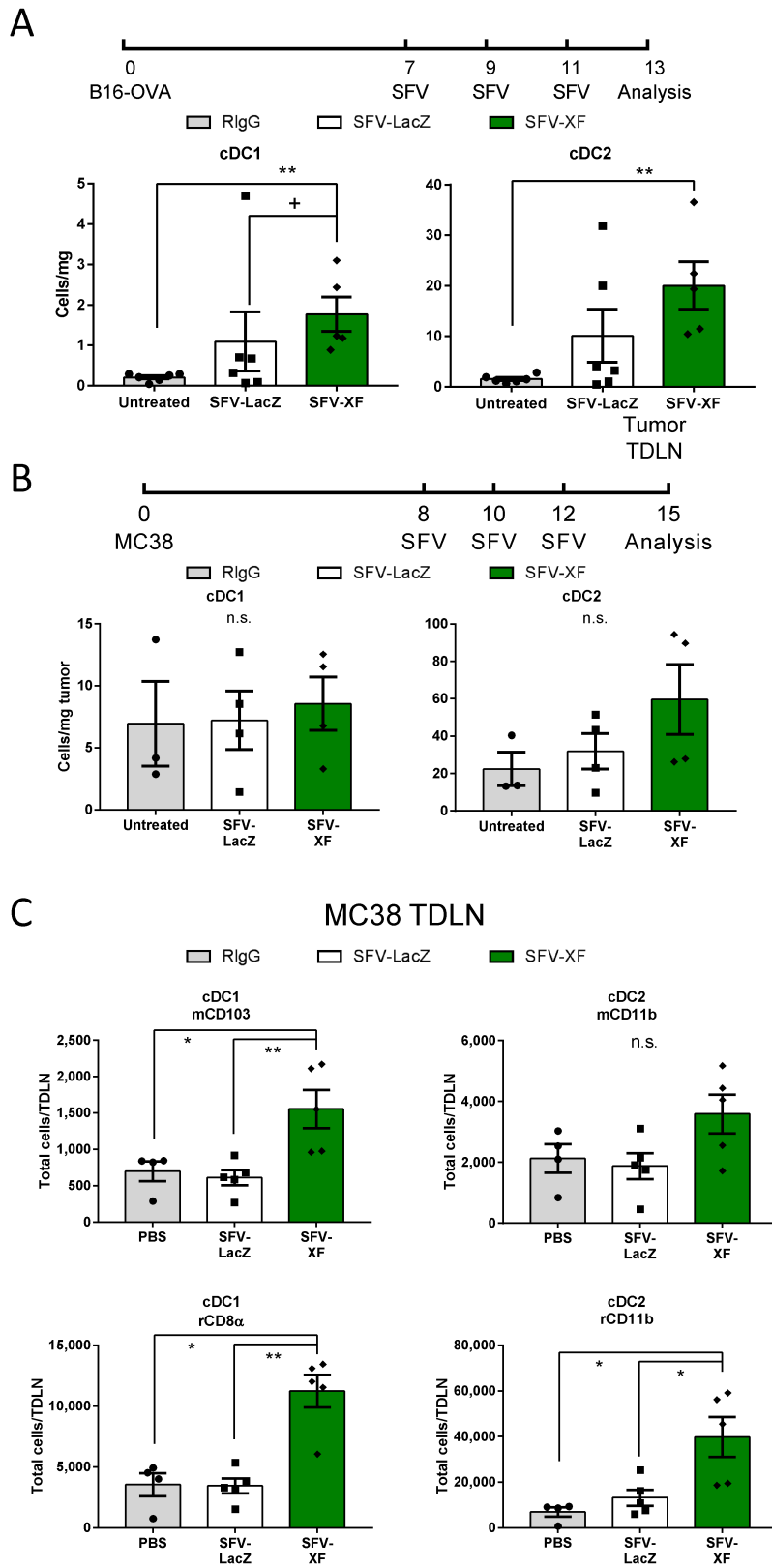
A

B16-OVA timeline: 0 (B16-OVA), 7 (SFV), 9 (SFV), 11 (SFV), 13 (Analysis)

Legend: RIgG, SFV-LacZ, SFV-XF

cDC1 **

Y-axis: Cells/mg (0–5)
X-axis: Untreated, SFV-LacZ, SFV-XF
Annotations: ** +

cDC2 **

Y-axis: (0–40)
X-axis: Untreated, SFV-LacZ, SFV-XF
Annotation: **

Tumor
TDLN

B

MC38 timeline: 0 (MC38), 8 (SFV), 10 (SFV), 12 (SFV), 15 (Analysis)

Legend: RIgG, SFV-LacZ, SFV-XF

cDC1 n.s.

Y-axis: Cells/mg tumor (0–15)
X-axis: Untreated, SFV-LacZ, SFV-XF

cDC2 n.s.

Y-axis: (0–100)
X-axis: Untreated, SFV-LacZ, SFV-XF

C

MC38 TDLN

Legend: RIgG, SFV-LacZ, SFV-XF

cDC1 mCD103 * **

Y-axis: Total cells/TDLN (0–2,500)
X-axis: PBS, SFV-LacZ, SFV-XF

cDC2 mCD11b n.s.

Y-axis: Total cells/TDLN (0–6,000)
X-axis: PBS, SFV-LacZ, SFV-XF

cDC1 rCD8α * **

Y-axis: Total cells/TDLN (0–15,000)
X-axis: PBS, SFV-LacZ, SFV-XF

cDC2 rCD11b * *

Y-axis: Total cells/TDLN (0–80,000)
X-axis: PBS, SFV-LacZ, SFV-XF

Intratumoral immunotherapy with XCL1 and sFlt3L encoded in recombinant Semliki Forest Virus-derived vectors fosters dendritic cell-mediated T cell cross-priming

Alfonso R. Sanchez-Paulete, Alvaro Teijeira, Jose I. Quetglas, et al.